Journal of Hazardous Materials B129 (2006) 164–170

Journal of Hazardous Materials

www.elsevier.com/locate/jhazmat

Characterization of the hydrothermally synthesized nano-TiO_2 crystallite and the photocatalytic degradation of Rhodamine B

Meltem Asiltürk [a], Funda Sayılkan [b], Sema Erdemoğlu [a], Murat Akarsu [c], Hikmet Sayılkan [b,*], Murat Erdemoğlu [d], Ertuğrul Arpaç [e]

[a] *Inönü University, Faculty of Arts and Science, Department of Chemistry, 44280 Malatya, Turkey*
[b] *Inönü University, Faculty of Education, Department of Science, 44280 Malatya, Turkey*
[c] *Institute für Neue Materialien, D-66123 Saarbrücken, Germany*
[d] *Inönü University, Faculty of Engineering, Department of Mining Engineering, 44280 Malatya, Turkey*
[e] *Akdeniz University, Faculty of Arts and Science, Department of Chemistry, 07100 Antalya, Turkey*

Received 27 April 2005; received in revised form 8 August 2005; accepted 20 August 2005
Available online 26 September 2005

Abstract

Pure anatase-TiO_2 nanoparticles with 8 nm average crystallite size was synthesized hydrothermally at 200 °C in 2 h. The structural and physicochemical properties of nano-TiO_2 were determined by powder XRD, FT-IR, BET and SEM analyses. The behavior of anatase nano-TiO_2 in catalytic degradation of Rhodamine B (RB) dye in transparent nano-TiO_2 sol under UV-light was examined as a function of irradiation power of UV-light, irradiation time, amount of nano-TiO_2 and initial RB concentration in the sol. Rhodamine B was fully degraded with the catalysis of the nano-TiO_2 in a short time as low as 60 min. Photocatalytic activity of the nano-TiO_2 for degradation of RB was compared with Degussa P-25 at optimum catalysis conditions determined for the nano-TiO_2. It was found that, when compared to Degussa P-25, the nano-TiO_2 could be repeatedly used with increasing photocatalytic activity. It was found that the photodegradation obeys the pseudo first-order reaction kinetics with the rate constant of 0.0658 min^{-1}, and the half period $t_{1/2}$ was 10.53 min.

Keywords: Nano-titania; Hydrothermal process; Photodegradation; Rhodamine B

1. Introduction

One of the major sources of environmental contamination is dyestuff that mainly comes from the textile and photographic industries [1–3]. Within the overall category of dyestuffs, Rhodamine B dye (RB), one of the most common xanthene dyes, is famous for its good stability as dye laser materials [4]. It has become a common organic pollutant, so the photodegradation of RB is important with regard to the purification of dye effluents. Photocatalytic degradation of several organic contaminants using large band gap semiconductor particles (such as TiO_2, ZnO and WO_3) have been studied extensively [3,5,6]. These contaminants present in an aqueous suspension of TiO_2 can be degraded with ultraviolet and visible light [7–9]. As one of the most popular photocatalyst, TiO_2 particle has long been investigated in environmental purification, decomposition of dyes in wastewater [10–12]. Anatase, brookite and rutile are three crystalline forms of TiO_2 and anatase-TiO_2 has attracted more attention for its vital use as pigments [13], gas sensors [14], catalysts [15,16], photocatalysts [17–19] in response to its application in environmental related problems of pollution control and photovoltaics [20]. The catalytic and other properties of these materials strongly depend on the crystallinity, surface morphology, particle size and preparation methods. The increased surface area of nanosized titania particles may prove beneficial for the decomposition of dyes in aqueous media. TiO_2 nanoparticles in powder have real advantages in relation to photocatalytic activity. In order to do this, different preparation processes have been reported, such as sol–gel process [21], hydrolysis of inorganic salts [22], ultrasonic technique [23], microemulsion or reverse micelles and hydrothermal process [24–26]. Polar or non-polar different solvents have been used in this process. Except the

* Corresponding author. Fax: +90 422 341 0042.
E-mail address: hsayilkan@inonu.edu.tr (H. Sayılkan).

0304-3894/$ – see front matter © 2005 Elsevier B.V. All rights reserved.
doi:10.1016/j.jhazmat.2005.08.027

hydrothermal process, in these processes, high calcination temperature above 450 °C is usually required to form regular crystal structure. However, in the meantime, the high temperature treatment can decline the surface area and lose some surface hydroxyl or alkoxide groups on the surface of TiO_2, which prevents easy dispersion. Thus, in this work, the hydrothermal process was selected to synthesize nanosize crystallized TiO_2 at low temperatures, which has been attractive to further improve the photocatalytic activity of TiO_2 as catalysts. Compared with the other TiO_2 powders, these TiO_2 nanoparticles have several advantages, such as fully pure anatase crystalline form, fine particle size with more uniform distribution and high-dispersion either in polar or non-polar solvents, stronger interfacial adsorption and easy coating on different supporting material. Moreover, the hydrothermal process including aqueous solvents as reaction medium is environmentally friendly since the reactions are carried out in a closed system, and the contents can be recovered and reused after cooling down to room temperature.

In this work, photocatalytic activity of a nano-TiO_2, which was hydrothermally synthesized at 200 °C within 2 h, was examined for degradation of RB in aqueous solutions and the results were compared with commercially available Degussa P-25 TiO_2 at optimum catalysis conditions determined previously for the nano-TiO_2.

2. Experimental

2.1. Materials

Titanium-iso-propoxide ($Ti(OPr^i)_4$, 97%) purchased from Alpha was used as titanium source for the preparation of TiO_2 photocatalyst. Hydrochloride acid from Merck (HCl, 37%) was used as catalyst for alkoxide hydrolysis. $Ti(OPr^i)_4$ and HCl were used without further purification. *n*-Propanol (Riedel de Haen, 99%) stored over molecular sieve (Fluka, 3 ÅXL8) was used as solvent. Rhodamine B dye purchased from a local textile factory was of analytical reagent grade and used without further purification, which its chemical formula is presented as,

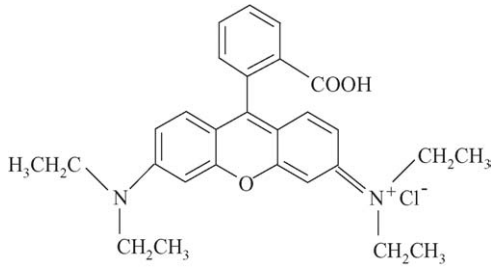

Degussa P-25 (Germany) TiO_2 with the BET surface area of $50\,m^2\,g^{-1}$ and anatase to rutile ratio of 80:20 was used as received. Deionized water was used for the hydrolysis of $Ti(OPr^i)_4$ and for preparation of all sols and solutions.

The crystalline phase of the hydrothermally synthesized TiO_2 nanoparticles was analyzed by X-ray powder diffraction (XRD) pattern obtained from Rigaku Geigerflex D Max/B diffractometer with Cu Kα radiation ($\lambda = 0.15418$ nm) in the region $2\theta = 10$–90° with a step size of 0.04°. The crystallite size of the anatase particle was calculated from the X-ray diffraction peak according to the Scherrer's equation. The surface morphology of TiO_2 was examined by a LEO EVO 40 Model scanning electron microscope (SEM). The BET surface area, average pore diameter and micropore volume of the nano-TiO_2 particle was calculated from the N_2 adsorption isotherm at liquid N_2 temperature using ASAP 2000 model BET analyzer. The sample was degassed at 130 °C for 4 h before N_2 adsorption. Pore size distribution of nano-TiO_2 was computed by DFT plus method.

Dye concentration in the solutions and mixtures before, during and after UV-irradiation was measured by a Schimadzu 1601 model UV–vis spectrophotometer. C and H elements in the nano-titania particle were analyzed by using element analyzer. UV-irradiation was carried out by a Solar Box 1500 model radiation unit with Xe-lamp and a controller to change the irradiation time and power input from 390 to 1100 $W\,m^{-2}$.

2.2. Preparation of nanocrystalline TiO_2 and photodegradation experiments

$Ti(OPr^i)_4$ was dissolved in *n*-propanol. After stirring for 5 min at ambient temperature, a *n*-propanol–hydrochloride acid mixture was dropwise added into alkoxide solution by burette at the rate of $1\,ml\,min^{-1}$. After stirring for 5 min, the mixture of water–*n*-propanol was added into the last solution dropwise by burette at the same rate. The mixture was stirred at ambient temperature for 10 min. Sol-solution was then transferred into a stainless steel Teflon-lined autoclave and heated at 200 °C for 2 h. The mole ratio of $H_2O/Ti(OPr^i)_4$ and $HCl/Ti(OPr^i)_4$ were 2 and 0.2, respectively. The as-obtained powders were separated through centrifugation and dried in a vacuum sterilizer at 30 °C for 4 h. Thus, nanosized TiO_2 crystallite powder was obtained.

Before examining the photocatalytic activity for aqueous degradation of RB, TiO_2 sol was prepared. For this purpose, certain amount of TiO_2 was just mixed with deionized water without addition of any reagent, such as dispersants and the mixture was ultrasonicaly treated for 10–15 min. Meanwhile, self-dispersed and transparent nano-TiO_2 sol was obtained.

For photodegradation experiments, required volume of dye solution was added into the nano-TiO_2 sol. After the temperature-constant sample preparation procedure and stabilizing the UV-light at the necessary power ınput for 15 min, the nano-TiO_2/RB dye sol was poured into the glass reaction cell which has 12 separate sample compartments and one cover and the cell was immediately located in the Solar Box ready for UV-irradiation inducing the photochemical reaction to proceed. The nano-TiO_2 sol/RB solution was also transparent before and after the degradation procedure. The decomposition of RB was monitored by measuring the absorbency at 548 nm (λ_{max}) and degradation was quantified by detecting RB concentration (C) directly in the sol before, during and after UV-irradiation. No filtration or centrifuging was needed for the nano-TiO_2 sol/RB system after photocatalysis procedure and before UV–vis spectrophotometric analysis, since it was already self-dispersed and transparent, i.e. it does not contain any visible solid particles.

Photocatalytic activity of the nano-TiO_2 was compared with Degussa P-25 for degradation of RB at optimum catalysis conditions determined for the nano-TiO_2, except that Degussa P-25

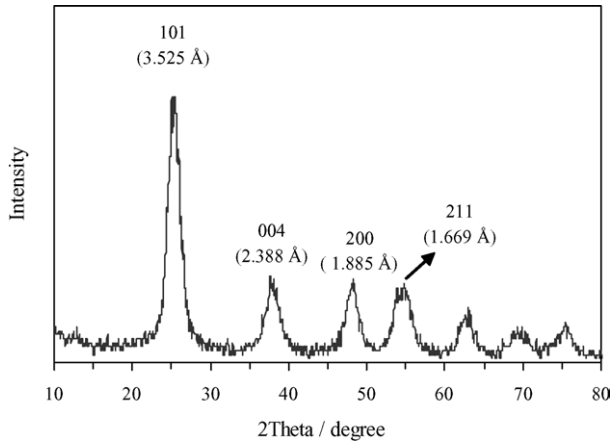

Fig. 1. XRD pattern of hydrothermally synthesized nano-TiO_2 powder (the numbers above the major peaks correspond to d_{hkl} spaces).

TiO_2 particles required to be removed from the system by filtration before UV–vis spectrophotometric analysis.

The nano-TiO_2 and Degussa P-25 were repetitively used to degrade 30 mg l^{-1} RB. After the first use, only Degussa P-25 was filtered and re-used. Then the so-used catalyst was employed to degrade a new 30 mg l^{-1} RB at the same conditions applied before. The process was repeated for four times.

3. Results and discussion

3.1. Characteristics of the TiO_2 photocatalyst

The crystalline phase of hydrothermally synthesized TiO_2 sample was analyzed by XRD, and its XRD pattern is shown in Fig. 1. When the XRD pattern was compared with PDF#21-1272 data files, it was found that all the sharp peaks belong to anatase-TiO_2 and rutile and brookite phases were not detected. Average crystallite size of TiO_2 was estimated according to the Scherrer's equation, $d_{hkl} = k\,\lambda/(\beta\cos(2\theta))$, where d_{hkl} is the average crystallite size (nm), λ the wavelength of the Cu Kα radiation applied ($\lambda = 0.154056$ nm), θ the Bragg's angle of diffraction, β the full-width at half maximum intensity of the peak observed at $2\theta = 25.3^\circ$ (converted to radian) and k is the constant usually applied as ~0.94. The average crystallite size of TiO_2 was estimated to be 8 nm. According to elemental analysis, it was determined that the TiO_2 contains 8.45% C and 2.05% H, which means that purity of the TiO_2 is about 90%.

Fig. 2 shows a typical SEM micrograph of as-synthesized nano-TiO_2. The particles are spherical in nature and the size of them seems less than 0.010 mm.

Some of the physicochemical properties of the synthesized TiO_2 is given Table 1. The BET surface area of the nano-TiO_2 is bigger but pore diameter, crystallite size and pore volume are smaller than Degussa P-25 with 63 m^2 g^{-1} specific surface area, 30 nm crystallite size and 0.06 ml g^{-1} pore volume [27] and the crystallite size is much lower than many other commercially available titanias. It is very-well known that the photocatalytic effect of a catalyst is dependent on the crystallite size and surface area. The smaller the particles, the larger will be its specific surface area and the higher photocatalytic activity.

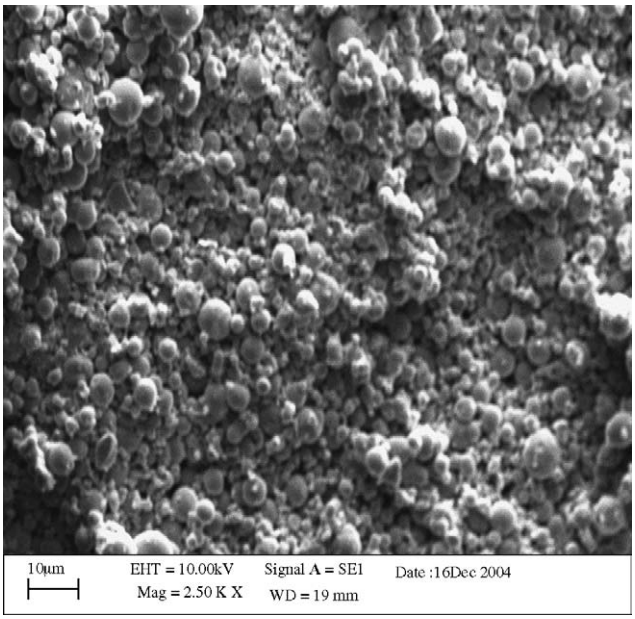

Fig. 2. Typical SEM microphotograph of hydrothermally synthesized nano-TiO_2 particle.

Table 1
Some physicochemical characteristics of the synthesized TiO_2

Property	
Crystalline type	Anatase
Crystallite size (nm)	8
TiO_2 content (%)	90
BET surface area (m^2 g^{-1})	114
Average pore diameter (nm)	2.12
Micropore volume (ml g^{-1})	0.023
Adsorption average pore diameter (Å)	21.3
Size of micropores (Å)	15
Size of mesopores (Å)	22–33

The FT-IR spectrum of nano-TiO_2 as-synthesized and dried at 30 °C is shown in Fig. 3. In the FT-IR spectrum, small bands at 2923 and 2792 cm^{-1}, small broad band at 2639 cm^{-1} are assigned as $-CH_2-$ and C–H stretching of aliphatic $-CH_2$ and $-CH_3$ groups bonded to Ti, respectively. C–H bending vibration was observed as a sharp band at 1407 cm^{-1}. Ti(O–C) vibration

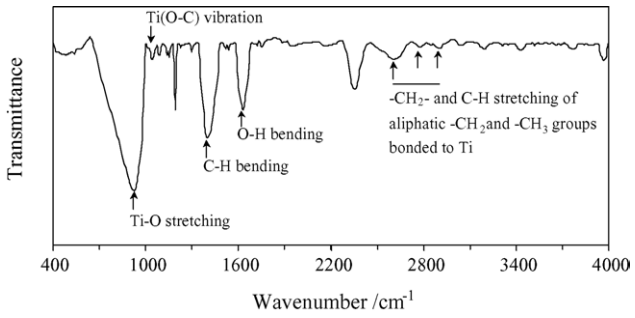

Fig. 3. Typical FT-IR spectrum of as-synthesized nano-TiO_2 particle dried at 30 °C.

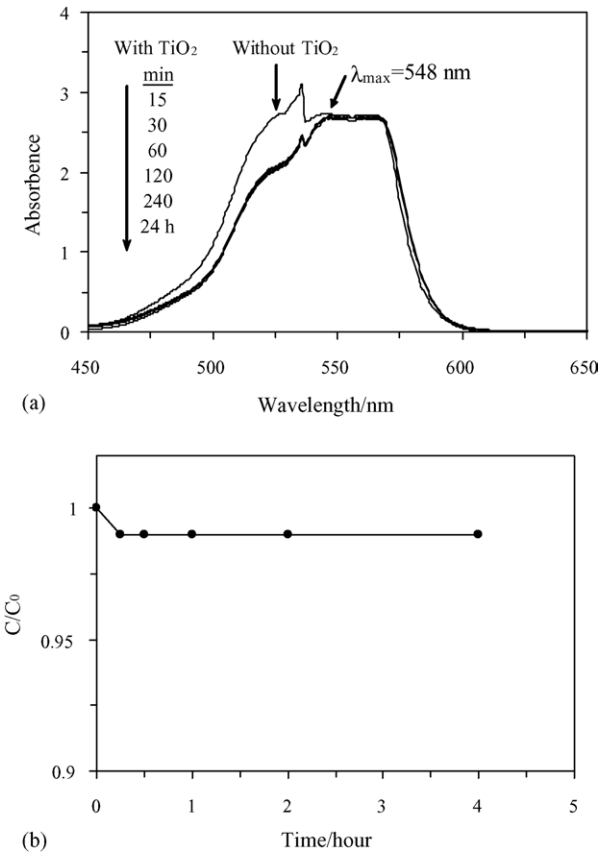

Fig. 4. (a) Time dependent variation in the absorbency and (b) adsorption of Rhodamine B in the nano-TiO_2 sol kept in the dark.

was observed as a small band at 1053 cm^{-1}. The O–H bending vibration was observed as a weak band close to 1638 cm^{-1}. The sharp band observed at 930 cm^{-1} was attributed to Ti–O stretching vibration.

3.2. Photocatalytic tests

The strong pre-adsorption of the RB on the TiO_2 surface is an important phenomenon for an efficient charge transfer, and not only does it affect the photodegradation rate, but also changes the photocatalytic mechanism. For this reason, before examining the photocatalytic activity of TiO_2 as a catalyst for degradation of RB, adsorption tests were carried out by keeping 25 ml of sol in its natural pH, and containing RB (C_0 = 30 mg l^{-1}) and 1 wt.% TiO_2 in the dark at room temperature. Fig. 4a shows the UV–vis absorption spectra of RB in TiO_2 sol, which are changing with the soaking time. The aqueous solution of RB (30 mg l^{-1}) shows a major absorption band at 548 nm in the absence of nano-TiO_2. The absorbencies of the TiO_2/RB sols decreased slightly after keeping 15 min in the dark, reflecting the extent of adsorption of RB on TiO_2. Fig. 4b shows the change of C_0/C with soaking period, where C_0 and C designate the concentrations of RB before and after treatment in the dark, respectively, and estimated from absorbance at the λ_{max} wavelength of RB. This indicates that maximum 1.0% of RB could be adsorbed onto TiO_2 within 15 min and the adsorbance did not changed with the prolonged soaking time. Therefore, from now on, all TiO_2/RB sols to be subjected to irradiation were soaked for 15 min in the dark.

The degradation of RB was investigated by using the hydrothermally synthesized nano-TiO_2 crystalline as catalyst under UV-irradiation. The UV–vis spectrum variation of RB catalyzed by TiO_2 under different irradiation times is shown in Fig. 5a. Normalized concentration variations with irradiation power, amount of nano-TiO_2 in the sol and initial RB concentration in the nano-TiO_2 sol are also shown in Fig. 5b–d, respectively. Table 2 briefly summarizes the experimental conditions for each factor affecting the photocatalytic degradation of RB and optimum conditions determined.

Shown in Fig. 5a is the effect of irradiation time on RB degradation. The color of TiO_2/RB sol changed to colorless with increasing UV-irradiation time, which indicated the degradation of RB. The experiments, which were repeated minimum three times showed that the absorbance value corresponding to 548 nm increases as the irradiation time was increased from 10 to 30 min. However, with the increasing irradiation time from 30 to 60 min, the absorption decreased gradually to a value near zero. The increase in the absorbance from 10 to 30 mg l^{-1} may be explained by the intermediate products of degrading RB absorbing UV–vis light at the wavelength region of RB. The reaction rate decreases with irradiation time since it follows apparent first-order kinetics and additionally a competition for degradation may occur between the reactant and the intermediate products. The slow kinetics of dyes degradation after certain time limit is due to: (a) the difficulty in converting the N-atoms of dye into oxidized nitrogen compounds [28], (b) the slow reaction of short chain aliphatics with $OH^{\bullet}$ radicals and (c) the short life-time of photocatalyst because of active sites deactivation by strong by-products deposition (carbon, etc.) [29]. With the increasing irradiation power up to 770 W m^{-2} (Fig. 5b), final RB concentration decreased immediately to a value near zero. With 690 W m^{-2}, no significant concentration was detected. Fig. 5b indicates that 60 min of irradiation time is adequate for complete degradation of 30 mg l^{-1} RB

Table 2
The values of experimental conditions for factors investigated for photodegradation of Rhodamine B by the catalysis of hydrothermally synthesized nano-TiO_2

Factor	Irradiation time	Irradiation power	Amount of nano-TiO_2	Rhodamine B concentration	Optimum value
Irradiation time (20–60 min)[a]	–	60	60	60	60
Irradiation power (450–940 W m^{-2})[a]	690	–	770	770	770
Amount of nano-TiO_2 (0.25–1 wt.%)[a]	1	1	–	0.25	0.25
Rhodamine B concentration (20–60 mg l^{-1})[a]	30	30	30	–	30

[a] The range studied during the examining of corresponding factor.

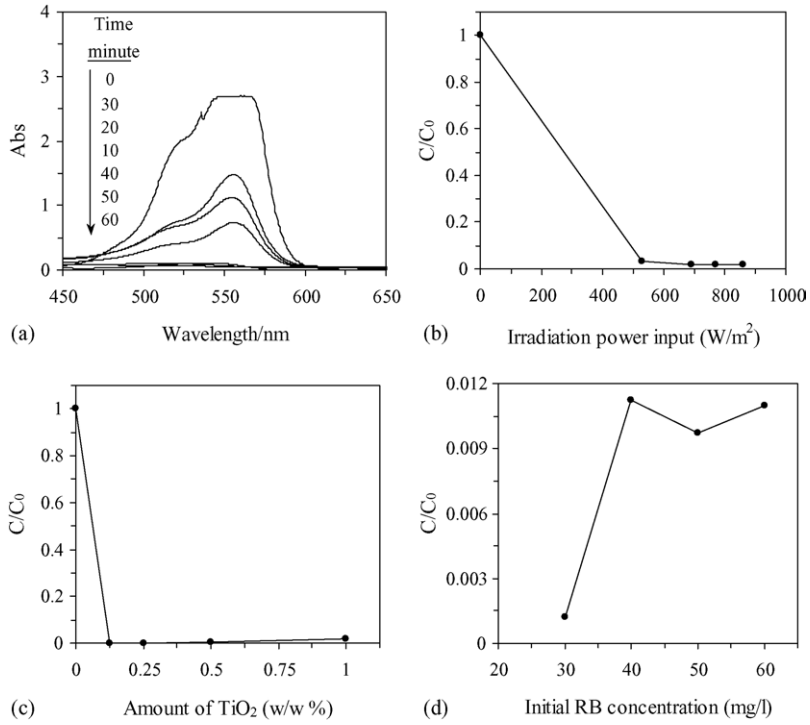

Fig. 5. Change in the absorbance spectra of Rhodamine B in the nano-TiO_2 sol with irradiation time (a) and normalized concentration variation of Rhodamine B with irradiation power input (b), amount of nano-TiO_2 (c) and initial Rhodamine B concentration (d).

in 1 wt.% nano-TiO_2 sol at 690 W m^{-2} irradiation power. The effect of light intensity on the kinetics of the photocatalysis process has been explained as (a) at lower light intensities like 0–20 mW cm^{-2}, the rate would increase linearly with increasing light intensity [30], (b) at intermediate increasing light intensities beyond a certain value like 25 mW cm^{-2}, the rate would depend on the square root of the light intensity [31] and (c) at high light intensities, the rate is independent of light intensity. At increased light intensity electron–hole pair separation competes with recombination, thereby causing lower effect on the reaction rate. Some researches observed that the enhancement of the rate of degradation as the light intensity increased was also observed [32–36]. The efficiency increases monotically with increasing light power; meanwhile, this dependency is not linear as revealed by a regression analysis. It is hoped that kinetic modeling and mechanistic studies will elucidate the effect of the light intensity, as well as the other ones, on the process efficiency. In our work, the degradation rate was increased with increased light power. This can be due to the absence of electron–hole recombination at higher light intensity like 690 W m^{-2}. It is also known that, at increased light intensities, electron–hole recombination causes lower effects on the reaction rate.

In order to avoid unnecessary excess catalyst and also to ensure total absorption of light photons for efficient photomineralization, usage of the optimum catalyst amount is important. The optimum amount of catalyst is found to be dependent on the initial solute concentration [29,31]. 0.25 wt.% TiO_2 in sol easily catalyzes the photooxidation of 30 mg l^{-1} RB just in 60 min (Fig. 5c). Photodegradation rate of RB decreases with the amount of the catalyst increases. This may be due to the decrease in the percentage of degradation at higher catalyst loading may be due to deactivation of activated molecules by collision with ground state molecules [32]. Shielding by TiO_2 may also take place

$$TiO_2{}^* + TiO_2 \rightarrow TiO_2{}^{\#} + TiO_2$$

where $TiO_2{}^*$ is the TiO_2 with active species adsorbed on its surface and $TiO_2{}^{\#}$ is the deactivated form of TiO_2 [32]. Agglomeration and sedimentation of the TiO_2 particles have also been reported [34]. In this condition, parts of the catalyst surface become unavailable for photon absorption and dye adsorption, thus bringing little stimulation to the catalytic reaction. On the contrary, continuous increase of the photocatalytic degradation rate of Reactive Black 5 was found up to 3500 mg l^{-1} TiO_2 [35]. The crucial concentration depends on the geometry, the working conditions of the photoreactor, the power and wavelength of UV-lamp.

The color of cream-colored TiO_2/RB sol changed to yellow with increasing initial RB concentration which indicated that photocatalytic activity of the 0.25 wt.% nano-TiO_2 was limited to almost 30 mg l^{-1} RB concentration (Fig. 5d). The concentration of aqueous solution of dye has a significant effect on the degradation rates. The higher the concentration, the lower the rate of degradation. This negative effect can be commented as follows: (a) when the dye concentration increases the amount of dye adsorbed on the catalyst surface increases. The increase in dye concentration also decreases the path length of photon entering the dye solution. At high dye concentration a significant amount of solar light may be absorbed by the dye molecules rather than the catalyst and this may also reduce the catalytic

Table 3
Comparison of the changes in the degradation times of the nano-TiO_2 and Degussa P-25

Catalyst	Degradation time (min)			
	First use	Second use	Third use	Fourth use
The nano-TiO_2	60	60	50	30
Degussa P-25	60	60	100	100

efficiency. Consequently, the degradation efficiency of the dye decreases as the dye concentration increases. (b) It is generally noted that the degradation rate increases with the increase in dye concentration to a certain level and a further increase in dye concentration leads to decrease the degradation rate of the dye [33,37]. The rate of degradation relates to the probability of $OH^{\bullet}$ radicals formation on the catalyst surface and to the probability of $OH^{\bullet}$ radicals reacting with dye molecules. As the initial concentrations of the dye increase the probability of reaction between dye molecules and oxidizing species also increases, leading to an enhancement in the decolorization rate. On the contrary, the degradation efficiency of the dye decreases as the dye concentration increases further. The presumed reason is that at high dye concentrations the generation of $OH^{\bullet}$ radicals on the surface of catalyst is reduced since active sites are covered by dye ions. Another possible cause for such results is the UV-screening effect of the dye itself. At a high dye concentration, a significant amount of UV may be absorbed by the dye molecules rather than the TiO_2 particles and that reduces the efficiency of the catalytic reaction because the concentrations of $OH^{\bullet}$ and $O_2^{\bullet -}$ decrease [34,35,38–42].

Since non-removability of the nano-TiO_2 from the sol seems like a disadvantage, reuse of the same sol for degradation of freshly added dye was also investigated. For this purpose, dye was again and again added to the nano-TiO_2 sol and Degussa P-25 suspension, after complete mineralization of the dye was attained.

Degussa P-25 was filtered after being used and then it was reused in the degradation of RB in the residual water from the former degradation process at the same optimum photodegradation conditions determined for the nano-TiO_2. Table 3 gives the photocatlysis times consumed until complete decolorization was observed during the reuse of the nano-TiO_2 and Degussa P-25. As seen from Table 3, much time was consumed when Degussa P-25 was used. Moreover, after the second use, the photocatalytic activity of Degussa P-25 decreased, whereas the nano-TiO_2 showed an increased activity (i.e. degradation time decreased when the same nano-TiO_2 sol was reused).

It was observed during the experiments that Degussa P-25 adsorbs more dye than the nano-TiO_2, resulting with a decrease in degradation rate. This may be due to high pore volume and pore diameter of the Degussa P-25. Moreover, as the amount of dye adsorbed on the surface of catalyst increases, thereby the active sites may be covered with dye ions, formation of $OH^{\bullet}$ radicals decreases. Higher dye adsorption of Degussa P-25 was also observed at the repeated usage. However, it was not measured, amount of Cl^- ions adsorbed onto Degussa P-25, which

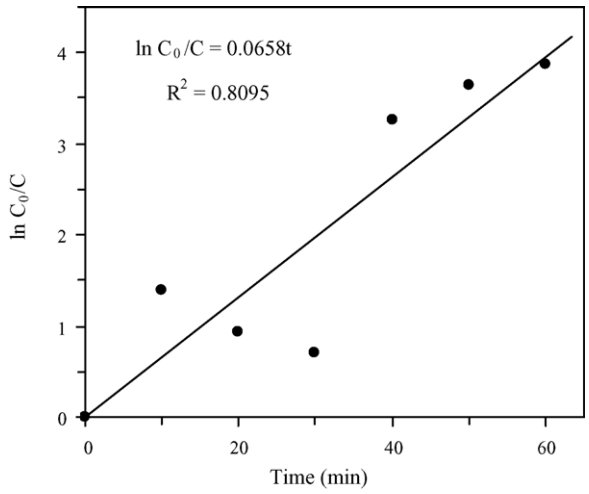

Fig. 6. The pseudo first-order reaction kinetics curve for photodegradation of Rhodamine B with the catalysis of nano-TiO_2, as obtained by re-plotting Fig. 5a in the $\ln(C_0/C)$-t coordinates.

generate as a result of mineralization of RB, may be more less than the nano-TiO_2, mainly depending on the lower surface area of Degussa P-25.

The equilibrium concentration data obtained from Fig. 5a were re-plotted in the $\ln(C_0/C)$-t coordinates (Fig. 6). It was observed that the photodegradation of RB simply follows the pseudo first-order reaction equation, $\ln(C_0/C) = kt$, where C_0 and C are the concentrations RB before and after the photoirradiation (mg l^{-1}), t the time (min) and k is the apparent reaction rate constant (min^{-1}). For RB with an initial concentration of 30 mg l^{-1} in 1 wt.% TiO_2 sol, the value of k is determined as 0.0658 min^{-1}. The half period, $t_{1/2}$, of RB was found to be 10.53 min by using the calculated parameter.

4. Conclusions

Pure TiO_2 with an 8 nm crystallite size was synthesized hydrothermally at 200 °C in 2 h. Anatase was the only crystalline phase in the nano-TiO_2 powder. The activity of the synthesized anatase-TiO_2 in catalytic degradation of Rhodamine B dye under UV-light was examined and found that it is a very efficient catalysis for complete degradation of higher concentrations of Rhodamine B in very short irradiation times.

Oxidation conditions were determined for photocatalytic degradation of Rhodamine B. Repeatedly usage of the synthesized catalyst was compared with Degussa P-25 and it was found that the nano-TiO_2 showed higher photocatalytic activity than Degussa P-25, even after the fourth use.

For initial concentration of 30 mg l^{-1} RB in 1 wt.% TiO_2 sol, the apparent reaction rate constant was 0.0658 min^{-1} and the half period of RB degradation was nearly 10.53 min.

Acknowledgement

The authors gratefully acknowledge the financial support of İnönü University, Turkey (BAPB-2004/01).

References

[1] A. Fujishima, K. Hashimoto, T. Wanatabe, TiO_2 Photocatalysis Fundamentals and Applications, BKC Inc., Tokyo, 1999.
[2] W.C. Tincher, Text. Chem. Color. 21 (1989) 23.
[3] M.R. Hoffmann, S.T. Martin, W.Y. Choi, D.W. Bahnemann, Chem. Rev. 95 (1995) 69.
[4] K. Vinodgopal, D.E. Wynkoop, P.V. Kamat, Environ. Sci. Technol. 30 (1996) 1660.
[5] D. Yu, R. Cai, Z. Liu, Spectrochim. Acta Part A 60 (2004) 1617.
[6] A. Sclafani, L. Palmisano, Solar Energy Mater. Solar Cells 51 (1998) 203.
[7] F.L. Zhang, J.C. Zhao, L. Zang, et al., J. Mol. Catal. A: Chem. 120 (1997) 173.
[8] P. Qu, J. Zhao, T. Shen, J. Mol. Catal. A: Chem. 129 (1998) 257.
[9] T.X. Wu, G.M. Liu, J.C. Zhao, J. Phys. Chem. B 102 (1998) 5845.
[10] A. Fujishima, K. Honda, Nature 238 (1972) 37.
[11] E. Pelizetti, C. Minero, Electrochim. Acta 38 (1993) 47.
[12] T. Hisanaga, K. Harada, K. Tanaka, J. Photochem. Photobiol. A 54 (1990) 113.
[13] J.G. Balfour, Technological Applications of Dispersions, Marcel Dekker, New York, 1994.
[14] Y.C. Yeh, T.T. Tseng, D.A. Chang, J. Am. Ceram. Soc. 72 (1989) 1472.
[15] C.G. Bond, S.F. Tahir, Appl. Catal. 71 (1991) 1.
[16] P.S. Awati, S.V. Awate, P.P. Shah, V. Ramaswamy, Catal. Commun. 4 (2003) 393.
[17] A. Hagfeldt, M. Gratzel, Chem. Rev. 95 (1995) 49.
[18] Y.H. Hsien, C.F. Chang, Y.H. Chen, S. Cheng, Appl. Catal. B 31 (2001) 241.
[19] C. Lizama, J. Freer, J. Baeza, H.D. Mansilla, Catal. Today 76 (2002) 235.
[20] N. Serpane, J. Texier, A.V. Emeline, P. Pichat, H. Hidaka, J. Zhao, J. Photochem. Photobiol. A 136 (2000) 145.
[21] G. Colon, M.C. Hidalgo, J.A. Navio, Catal. Today 76 (2002) 91.
[22] Y. Zhang, G. Xion, N. Yao, W. Yang, X. Fu, Catal. Today 68 (2001) 220.
[23] X.M. Wu, L. Wang, Z.C. Tan, G.H. Li, S.S. Qu, J. Solid State Chem. 156 (2001) 220.
[24] E. Vigil, J.A. Ayllon, A.M. Peiro, R.R. Clemente, Langmuir 17 (2001) 891.
[25] H. Zhang, M. Finnegan, J.F. Banfield, Nano Lett. 1 (2001) 81.
[26] X. Ju, P. Huang, N. Xu, J. Shi, J. Membr. Sci. 202 (2002) 63.
[27] J.G. Yu, M.H. Zhou, B. Cheng, H.G. Yu, X.J. Zhao, J. Mol. Catal. A: Chem. 227 (2005) 75.
[28] J. Bandara, V. Nadtochenko, J. Kiwi, C. Pulgarin, Water Sci. Technol. 35 (1997) 87.
[29] I.K. Konstantinou, T.A. Albanis, Appl. Catal. B: Environ. 49 (2004) 1.
[30] D.F. Ollis, E. Pelizzetti, N. Serpone, Environ. Sci. Technol. 25 (1991) 1523.
[31] J.M. Hermann, Catal. Today 53 (1999) 115.
[32] B. Neppolian, H.C. Choi, S. Sakthivel, B. Arabindoo, V. Murugesan, Chemosphere 46 (2002) 1173.
[33] S. Sakthivel, B. Neppolian, M.V. Shankar, B. Arabindoo, M. Palanichamy, V. Murugesan, Solar Energy Mater. Solar Cells 77 (2003) 65.
[34] C.M. So, M.Y. Cheng, J.C. Yu, P.K. Wong, Chemosphere 46 (2002) 905.
[35] L.B. Reutergarth, M. Iangphasuk, Chemosphere 35 (1997) 585.
[36] T. Sauer, G.C. Neto, H.J. Jose, R.F.P.M. Moreira, J. Photochem. Photobiol. A: Chem. 149 (2002) 147.
[37] M. Saquib, M. Munner, Desalination 155 (2003) 255–263.
[38] W.Z. Tang, H. An, Chemosphere 31 (1995) 4157.
[39] J. Grzchulska, A.W. Morawski, Appl. Catal. B: Environ. 36 (2002) 45.
[40] N. Daneshvar, D. Salari, A.R. Khataee, J. Photochem. Photobiol A: Chem. 157 (2003) 111.
[41] A. Mills, R.H. Davis, D. Worsley, Chem. Soc. Rev. 22 (1993) 417.
[42] I. Poulios, I. Aetopoulou, Environ. Technol. 20 (1999) 479.